www.springer.com/41230
https://doi.org/10.1007/s41230-023-2095-5
Research & Development
Vol. 20 No. 5 September 2023
CHINA FOUNDRY

Effects of macrosegregation on mechanical and tribological properties of squeeze casting immiscible bearing alloys

Ming Xu[1], *Yan-guo Yin[1], Cong-min Li[1], Guo-tao Zhang[2], and Cong-chong Duan[3]
1. Institute of Tribology, School of Mechanical Engineering, Hefei University of Technology, Hefei 230002, China
2. School of Mechanical Engineering, Anhui University of Technology, Maanshan 243002, Anhui, China
3. Anhui Yihui New Material Co., Ltd., Hefei 230000, China

Abstract: The macrosegregation behaviors of Al-Sn-Cu ternary immiscible alloy castings and their effects on mechanical and tribological properties were investigated. The results demonstrate that Sn and Cu segregate in the casting simultaneously, and the mass fraction of the two elements has a "U" shaped distribution. Significantly, positive and negative segregation occur in the casting, with positive segregation appearing on the top and lower surfaces and negative segregation on the remaining surfaces, with the 1/2 surface (hot node location) having the highest degree of negative segregation. Furthermore, the results of Vickers hardness, tensile strength, and elongation show that Sn and Cu cooperatively affect the mechanical properties of castings. The higher the mass fraction of Sn and Cu elements, the higher the hardness, the greater the tensile strength, and the better the elongation. The findings of the step-by-step loading tests demonstrate that the segregation of Sn and Cu significantly impacts the tribological characteristics of the castings. The higher the mass fraction of Sn and Cu on the sample surface, the better the tribological characteristics.

Keywords: squeeze casting; Al-Sn-Cu; macrosegregation; mechanical properties; tribological property
CLC numbers: TG146.21 **Document code:** A **Article ID:** 1672-6421(2023)05-443-09

1 Introduction

Aluminum (Al)-based sliding bearing alloys have become the most important material for medium- and light-load sliding bearings due to abundant resources and low cost. It is widely used in internal combustion engines, hydraulic gear pumps, reciprocating compressors, and aviation equipment. With the rapid advancement of the equipment industry, the comprehensive qualities of sliding bearing materials, such as the bearing capacity and tribological properties, have been continuously enhanced through constant innovation, improvement, and optimization. To futher improve the mechanical characteristics and tribological properties, many researchers have focused on adding Cu, Si, and other elements to the aluminum-based sliding bearing alloy matrix. Kong et al. [1] added Cu to Al-Sn alloys to enhance the fatigue strength of the material by boosting the solid solution-strengthening effect of the matrix. Belov et al. [2] investigated the influence of Si and Cu additions on the phase constitution, microstructure, and characteristics of Al-Sn alloys. The results indicate that the addition of 4% Cu significantly increases the hardness of the alloy. But, the electrical conductivity and manufacturability during cold rolling are decreased. Whereas, the Si increases the hardness and manufacturability during casting but decreases the electrical conductivity. Rusin et al. [3] investigated the influence of Cu on the mechanical and friction characteristics of Al-Sn sintered composites and discovered that the addition of 2%Cu have no effect on the macrostructure of the sintered Al-Sn-Cu alloy. However, when the Cu content increases to 2%, the composite strength and fexibility increase, and the Al-Sn-Cu composites under dry friction have greater wear strength than the Al-Sn composites. The microstructure, tensile properties, and wear resistance of Al-Sn-(Cu;Si) alloys were investigated by Felipe et al [4]. The results reveal that the Al-Sn-Cu ternary alloy with a coarser microstructure has better friction and wear characteristics, and a finer

***Yan-guo Yin**
Male, Professor. Research interests: Lead-free environment-friendly selflubricating materials, aviation lightweight materials, hydraulic key friction pair parts.
E-mail: abyin@sina.com
Received: 2022-06-28; Accepted: 2023-03-10

microstructure corresponds to better tensile properties, with the friction and tensile properties trending in opposing directions. While, the dendrite size does not affect the wear resistance of the Al-Sn-Si ternary alloy, but, the tensile strength dramatically improves when the dendrite size decreases. In general, the purpose of research on Al-Sn-Cu ternary alloys is to tackle the problem of uniform distribution of immiscible Sn element, expose the microstructure evolution during solidification, and analyze the friction, wear, and mechanical characteristics. However, there are few studies on the element segregation rule in the Al-Sn-Cu ternary alloy and its effects on mechanical and tribological properties.

It is well known that substantial segregation occurs during solidification due to the large miscibility gap in the Al-Sn-Cu ternary alloy. Some related research works on the control methods of Sn homogenization, such as stir casting [5-6], rapid solidification [6-7], vapor deposition method [8-9], electrochemical deposition method [10], mechanical alloying [11], alloying element addition [6, 12-13], and dense melt shearing method [14], have been develpoed. It can be observed that the optimization and innovation of forming processes can effectively alleviate the segregation phenomenon of the Sn element. The squeeze casting technique, as a novel method that combines the advantages of casting and forging, has been commonly employed in manufacturing high-quality castings. Squeeze casting technology can promote mechanical properties and decrease forming process defects such as cracks and porosity. However, segregation remains unavoidable in castings, and the segregation exhibits clear diversity when pressure is added [15-21]. Building upon previous research, this study focuses on investigating the segregation distribution of the immiscible element tin (Sn) and the solute element copper (Cu) in squeeze casting of the Al-Sn-Cu ternary alloy. The aim is to study the segregation behavior of Sn and Cu and the influence of the segregation behavior on the mechanical and tribological properties of castings under heat treatment. The experimental results, encompassing microstructural analysis, mechanical property testing, and tribological performance evaluation, serve as a basis for understanding and advancing the application of the Al-Sn-Cu ternary alloy.

2 Experiment

2.1 Materials and preparation

In the experiment, the designed composition (mass fraction, %) of the Al-Sn-Cu ternary alloy is shown in Table 1. The commercial-grade aluminum (99.7%), pure Sn (99.99%), and Al-50%Cu alloy were proportionally put into a resistance furnace and then was heated to 760 °C. After the alloy ingot was completely melted, the argon gas rotary injection method was used to refine and degas the molten alloy. The composition test was performed prior to pouring to confirm the homogeneity and consistency of the experimental materials. The castings were made using the direct squeeze casting procedure, as shown in Fig. 1. The 4,000 kN vertical extruder was used, as shown in Fig. 2(a). The upper and lower molds are shown in Figs. 2(b) and (c). Before pouring, the upper and lower molds were preheated to 200 °C and 180 °C, respectively. Then, the molten metal of 720 °C was poured into the lower mold. After that, the mold closure button was engaged quickly. The upper mold moved downward and the casting solidified under isostatic pressure. The specific pressure was 80 MPa and holding time was 25 s. Finally, the mold was returned to original position, and the casting was removed. The heat treatment process was that solution treated at 490 °C for 4 h, after quenching in cold water, the aging was carried out at 200 °C for 6 h.

Table 1: Main composition of experimental material Al-Sn-Cu

Composition	Sn	Cu	Fe	Al
wt.%	5	4	<0.2	Bal.

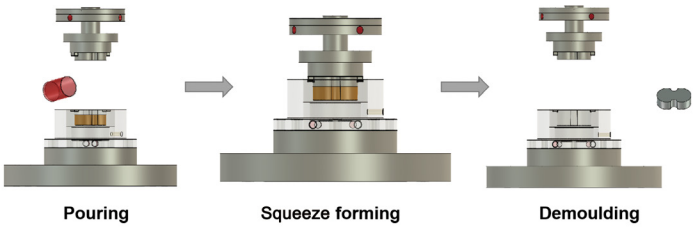

Fig. 1: Schematic diagram of squeeze casting experimental process

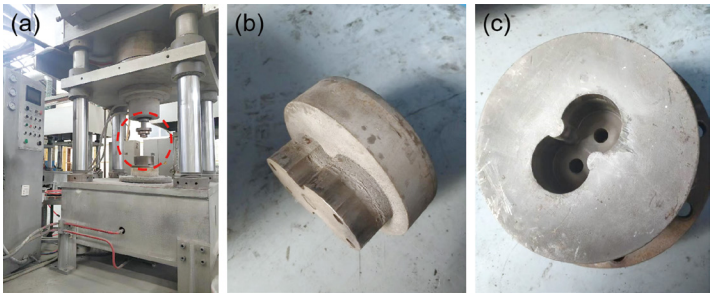

Fig. 2: Forming equipment and molds: (a) vertical extruder; (b) upper mold; (c) lower mold

2.2 Method

The squeeze cast specimen is in the shape of "8" with a height of 30±2 mm, as shown in Fig. 3(a). The upper and lower surfaces were milled to remove 2.5 mm each before being sliced by wire cutting and labeled as upper surface, 1/4 surface, 1/2 surface, 3/4 surface, and lower surface. As shown in Fig. 3(b), the thickness was 5 mm. After lathing, the compositions of each surface were identified using a German SPECTRO direct-reading spectrometer.

As indicated in Fig. 4(a), the detecting locations were numbered from 1 to 9. After grinding and polishing, the HV-1000A Vickers

hardness tester was used to measure hardness. The detection position was compatible with the composition detection point. A JSM-6490LV environmental scanning electron microscope (SEM) was used to analyze the microstructure, fracture morphology of tensile specimens, and wear marks of tribological test specimens, and INCA energy dispersive spectroscopy (EDS) was used to determine the alloy composition. Meanwhile, the intergranular phase distribution area fraction was calculated by Image-Pro Plus image analysis software. The phase constitution was analyzed using a Rigaku D/MAX2500VL/PC rotating target X-ray diffractometer. In order to test the mechanical properties, the sample was immediately divided into 5 pieces with a thickness of 5 mm, the position and size are shown in Fig. 4(b). The room temperature tensile testing was performed using a 10 t hydraulic universal testing machine with the tensile speed of 0.02 mm·s^{-1}.

The friction and wear test was performed using a custom-built HDM-20 end-face friction and wear tester. In experiment process, the casting was held in place and the anti-abrasive component was turned, as shown in Fig. 5. The abrasive pieces were made of Cr12 steel with a surface roughness of 0.2 μm. The experimental method of step loading was adopted. The initial axial load and loading amplitude was 100 N and 100 N·min^{-1}, respectively. The speed of rotation was 517 r·min^{-1} (linear speed was 1.0 m·s^{-1}). Lubrication was provided by dipping the sample in #32 mechanical oil. The friction factor and other statistics were collected by the testing equipment. When the oil coating between the mating surfaces was fully removed during the test, the friction coefficient significantly increased, and the temperature progressively increased. The experiment was terminated when the temperature reached 200 °C.

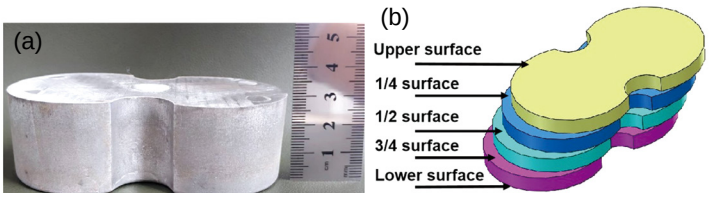

Fig. 3: Specimen diagram: (a) squeeze cast specimen; (b) section sampling diagram

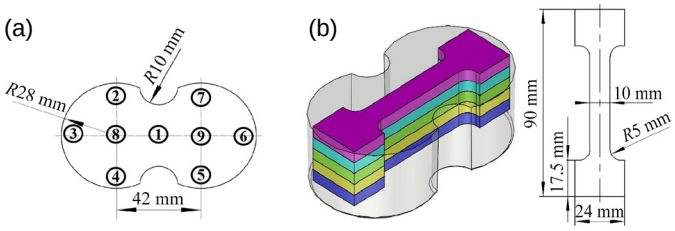

Fig. 4: Sampling diagram: (a) single chip component detecting location; (b) sampling position and size of tensile sample

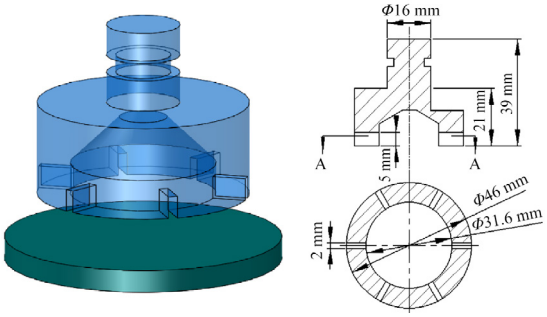

Fig. 5: Friction pair dimensions in friction and wear test

3 Results and discussion

3.1 Macrosegregation

Figure 6 shows the X-ray diffractometer (XRD) spectrum of the Al-Sn-Cu alloy prepared by squeeze casting process. The Al-Sn-Cu alloy is composed of α(Al), β(Sn), and Al_2Cu. During solidification, Sn is immiscible with liquid aluminum, and it mostly exhibits a network distribution at grain boundaries, as shown in Fig. 7. The α(Al) matrix is dark grey. The β(Sn) exhibits a dazzling white color and tends to aggregate into clusters at grain boundaries. A portion of the Cu element forms Al_2Cu, appearing as light gray irregular shapes distributed along the boundaries, while another portion dissolves into the Al matrix, dispersing uniformly.

Figure 8 depicts SEM images of the No. 1 position in Fig. 4 on various squeeze casting surfaces. The microstructure of the casting changes obviously from the upper surface to lower surface. In the upper surface, grains are small and homogeneously distributed, with incomplete grain boundaries, and the microstructure is evenly dispersed. The white β(Sn) and Al_2Cu dispersed throughout the grains are mostly granular and elongated, as shown in Fig. 8(a). This is primarily due to the high degree of supercooling produced by direct contact between the molten aluminum and the upper mold, which results in a rapid solidification rate and a fine and uniform grain structure. When pressure is directly applied to the upper surface, the activation energy is reduced, which increases the nucleation rate and refines the grain structure. Simultaneously, under pressure, the grain boundaries undergo compression, distortion, and interlinking, leading to the partial vanishing of grain

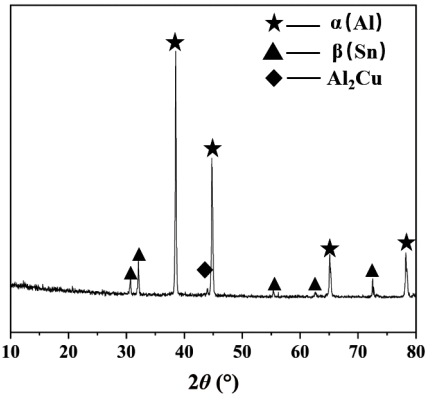

Fig. 6: XRD spectrum of squeeze casting process castings

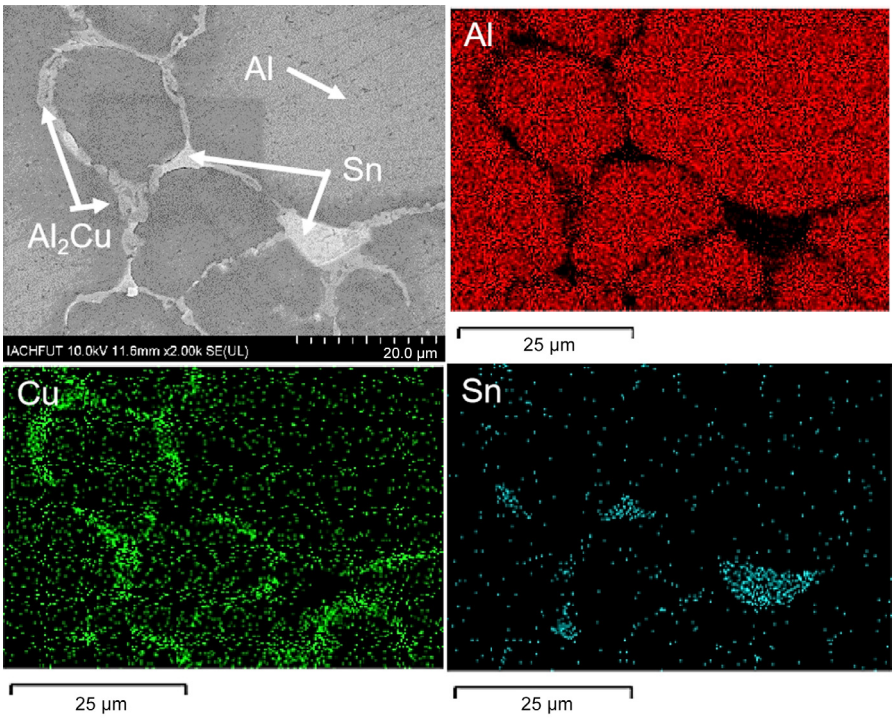

Fig. 7: EDS test results of microstructure composition of alloy

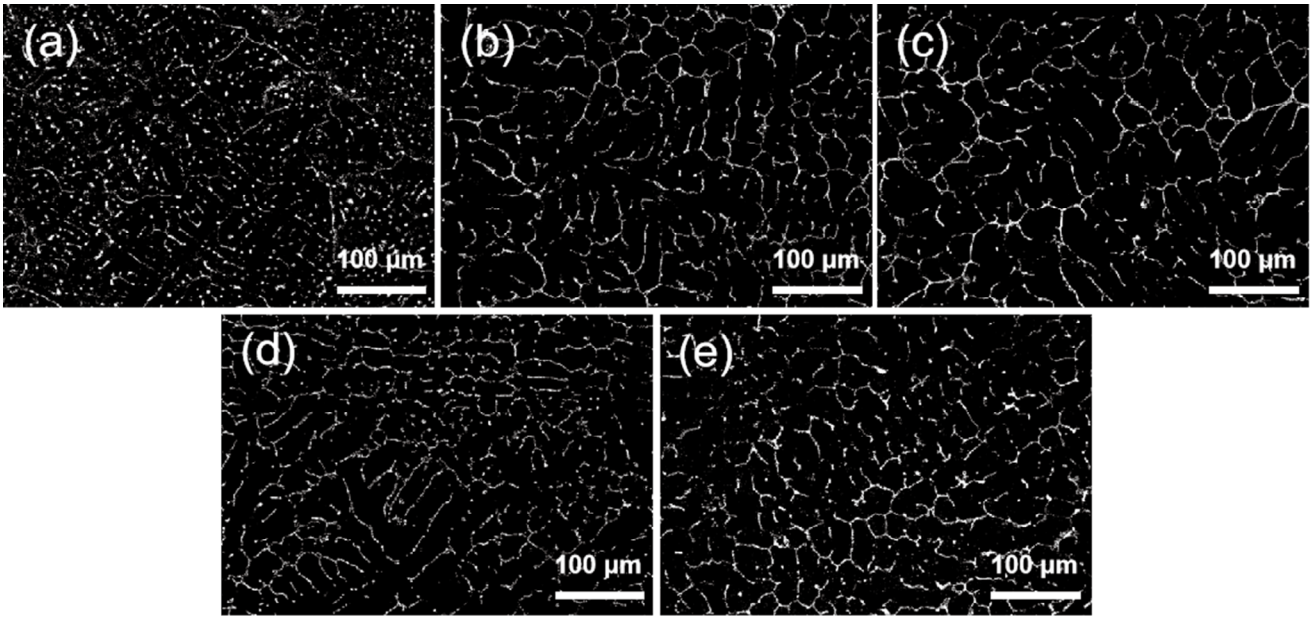

Fig. 8: SEM images of different surfaces of squeeze casting: (a) upper surface; (b) 1/4 surface; (c) 1/2 surface; (d) 3/4 surface; (e) lower surface

boundaries. This, in turn, results in the formation of granular and elongated morphologies of β(Sn) and dispersed Al_2Cu along the grain boundaries. The structure from the 1/4 surface to the lower surface has a discontinuous network structure. The grain evolves from fine to coarse to fine, and the 1/2 surface structure is the coarsest. When molten aluminum is put into the mold, it quickly solidifies and forms a thick shell. After the mold is closed, under the pressure condition, the solidification speed of the casting is faster, the solid-liquid coexistence zone becomes narrower, and the solidification mode tends to solidify layer by layer. The 1/2 surface is treated as the hot spot in this study. Due to the long solidification time, the microstructure at the hot spot is relatively coarse. Simultaneously, the mass fractions of the white β(Sn) and Al_2Cu phases change significantly in the thickness direction, which indicates that the macroscopic segregation of Sn and Cu occurs in the thickness direction during the squeeze casting process. As shown in Fig. 9, the segregation phenomena in the casting are further exposed. The area fraction of the second phase composed of white β(Sn) and Al_2Cu displays a "U" distribution in the thickness direction, which indicates that Sn and Cu are segregated in the casting's thickness direction.

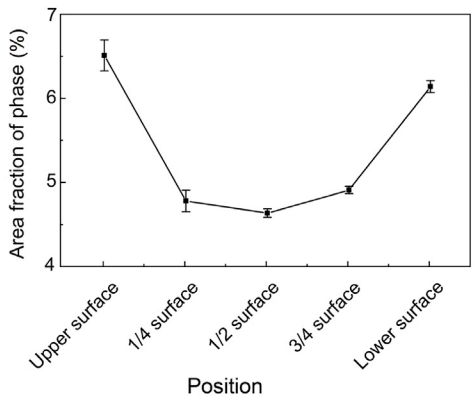

Fig. 9: Area fraction of β(Sn) and Al_2Cu distributed in different surfaces of casting

To investigate the composition segregation behavior in the Al-Sn-Cu ternary immiscible alloy, the composition of each casting surface was examined, and the segregation rate of Sn and Cu can be determined by Eq. (1) [22]:

$$\eta = \frac{C_i - C_0}{C_0} \quad (1)$$

where, η is the segregation rate of a specific portion of the casting, C_i is the mass fraction of a specific portion of the casting, and C_0 is the casting's average mass fraction (original composition mass fraction). There is no segregation when η=0. η<0 indicates negative segregation, and a lower negative value corresponds to a more severe negative segregation; η>0 indicates positive segregation, and a greater positive value corresponds to a more severe positive segregation. Table 2 displays the statistics and analytical results of Sn and Cu mass fractions detected on different surfaces. The results demonstrate that the casting contains both Sn and Cu macrosegregation. Positive and negative segregations concurrently exist with positive segregation on the top and lower surfaces and negative segregation on the remaining surfaces. Negative segregation at the 1/2 surface (hot node location) is the most significant. As demonstrated in Fig. 10, the Sn and Cu mass fractions have a "U"-shaped pattern. This is mostly because once the molten aluminum is poured into the mold, the Sn-rich liquid phase and Cu-rich liquid phase are excluded from the firstly solidified shell, which increases the Sn and Cu mass fractions in the remaining liquid phase. During the mold closure, the upper mold comes into direct contact with the molten aluminum, leading to the formation of a closed shell. According to the Clausius-Clapeyron equation [23], it is evident that changes in pressure significantly influence the solidification process:

$$\frac{\Delta T_f}{\Delta p} = \frac{T_f(V_1 - V_s)}{\Delta H_f} \quad (2)$$

where T_f is the equilibrium solidification temperature of the alloy, V_1 is the volume of the liquid phase, V_s is the volume of the solid phase, H_f is the latent heat of fusion, and p is the pressure on the alloy. With increasing pressure, the equilibrium solidification temperature T_f increase, degree of undercooling and solidification rate increase. The Sn-rich liquid phase and Cu-rich liquid phase on the top surface freeze before migrating. Under pressure, the closed shell layer undergoes continuous solidification towards the hot spot location. The Sn-rich and Cu-rich liquid phases, which have a high mass fraction, provide feeding to compensate for the firstly solidified volume contraction at the hot spot position. However, in the later stages of solidification, as the solidification shrinkage becomes concentrated at the hot spot location, the interdendritic feeding channel eventually closes, leading to the absence of residual liquid phase for feeding. Consequently, the application of pressure at the hot spot location induces a limited amount of plastic deformation within the solid phase, leading to the completion of the forced feeding process. This results in severe negative segregation of Sn and Cu at the hot pot position.

Table 2: Statistical results of Sn and Cu mass fractions detected on different surfaces

Element	Location	Position in Fig. 4									Average (%)	Segregation rate (%)
		1	2	3	4	5	6	7	8	9		
Sn	Upper surface	5.38	5.44	5.39	5.37	5.4	5.4	5.35	5.4	4.29	5.27	2.25
	1/4 surface	5.22	5.07	5.61	5.3	5.21	5.03	5.45	4.94	4.04	5.10	−1.05
	1/2 surface	4.82	5.2	5.01	5.13	4.93	5.29	5.09	5.28	3.99	4.97	−3.57
	3/4 surface	5.22	5.08	5	5.11	5.22	5.25	5.14	5.29	4.99	5.14	−0.27
	Lower surface	5.58	3.51	5.64	5.57	5.66	5.52	5.58	5.43	5.11	5.29	2.64
Cu	Upper surface	4.43	4.55	4.52	4.51	4.44	4.56	4.45	4.56	4.29	4.48	6.41
	1/4 surface	4.2	4.09	4.12	4.15	4.14	4.02	4.1	4.01	4.04	4.10	−2.61
	1/2 surface	3.72	3.93	3.93	3.98	3.7	3.91	3.9	3.92	3.99	3.89	−7.6
	3/4 surface	4.13	4.02	3.95	4.03	4.16	3.98	4.02	3.98	4.18	4.05	−3.8
	Lower surface	4.43	4.44	4.51	4.51	4.46	4.48	4.44	4.4	5.11	4.53	7.6

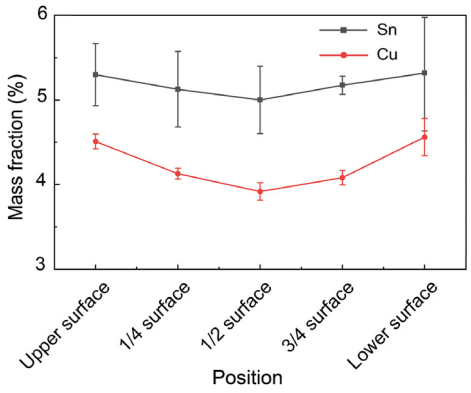

Fig. 10: Distribution of mass fractions of Sn and Cu at different surfaces

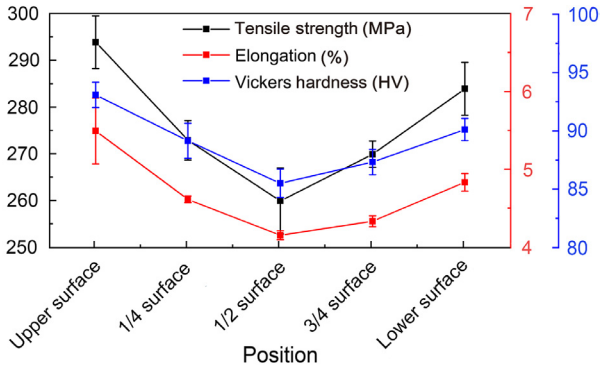

Fig. 11: Curves of tensile strength, elongation and Vickers hardness of different surfaces

3.2 Influence of segregation on mechanical properties

The results of Vickers hardness, tensile strength, and elongation are shown in Fig. 11. The Vickers hardness, tensile strength, and elongation drop firstly and subsequently rise from the upper to the lower surface. It can be found that this has the same "U-shaped" characteristics as the segregation distribution of Sn and Cu elements (Fig. 10). As a result, it is reasonable to infer that the distribution of Sn and Cu segregation affects the Vickers hardness, tensile strength, and elongation of the castings. The Al-Sn-Cu ternary immiscible alloy is mostly composed of α(Al), β(Sn), and Al_2Cu compounds. β(Sn) is a soft phase spread throughout the grain that easily splits the matrix, generates crack sources, and reduces the strength of the casting, whereas the Cu element strengthens the matrix, so the strength of the casting is the consequence of the combined influence of Sn and Cu. The element distribution law of Sn and Cu is closely connected to the strength change.

As it is known, solid solution and grain refinement are essential methods to increase the metal material strength. The Al-Sn-Cu alloy casting has been subjected to solid solution and aging heat treatment, scattered Cu atoms are precipitated in the α(Al) matrix [24], which enhances the alloy matrix's strength and hardness. The strength of Al-Sn-Cu alloy castings is spread in a "U" shape, which is mostly governed by the Cu segregation distribution. The upper surface has fine grains and a high Cu mass fraction, and the mechanical properties of the upper surface are excellent. The grain size significantly influences the slip behavior of the matrix. Finer grains, which possess a higher density of grain boundaries, effectively impede grain boundary sliding and enhance the strength. Therefore, in this experiment, both the solid solution strengthening of Cu and the refinement of grain size contribute to the strengthening of the matrix. While β(Sn) exerts a certain weakening effect on the matrix, the strengthening effect of Cu element is more significant. Consequently, the mechanical properties of castings exhibit a significant decline with the increase in Sn and Cu grain size, as well as the decrease in mass percentage. The Vickers hardness, tensile strength, and elongation of the half surface of the castings are reduced by 8.5%, 11.5%, and 24.4%, respectively.

Figure 12 shows fracture photographs of tensile specimens on different surfaces. The fracture on the upper surface is mostly a mixed fracture morphology of quasi-cleavage and ductile fracture. With a small amount of second phase, ripping edges and dimples are visible, indicating that the upper surface tensile specimen has greater elongation, as shown in Fig. 12(a). The EDS analysis results show that the second phase mainly consists of Sn, as shown in Fig. 13. Although the mass fraction of Sn is higher, the splitting effect of uniformly distributed small size Sn on the matrix is weakened and the tensile strength and plasticity are improved. The fracture analysis of the 1/4 surface tensile test bar, as depicted in Fig. 12(b), reveals the growth of a second phase at the fracture surface, accompanied by a decrease in dimples and tearing edges. The primary fracture modes observed are still quasi-cleavage and ductile fracture. Furthermore, the fracture morphology of the 1/2 surface tensile sample, as shown in Fig. 12(c), exhibits larger second phases and fewer dimples and tearing edges. Despite the low mass fraction of Sn element, the larger size of the second phase structure exerts a significant cleavage effect on the matrix, resulting in lower tensile strength and elongation. Comparatively, the reduction in second phases, along with the enhancement of tear edges and dimples, can be observed in the 3/4 surface, leading to improved tensile properties, as depicted in Fig. 12(d). The fracture modes observed on the bottom surface of the tensile test bar are a mixture of quasi-cleavage and ductile fracture, predominantly involving quasi-cleavage, as shown in Fig. 12(e). Notably, the lower presence of tear edges and dimples on the bottom surface contributes to lower tensile strength and plasticity compared to upper surface.

3.3 Influence of segregation on tribological properties

The Al-Sn-Cu alloy is considered a "soft and hard coordination" double friction pair material. In this context, the product of the end pressure (P) and the peripheral velocity (V) of the friction pair is a constant value that is determined by the material properties [25, 26]. To comprehensively evaluate the tribological characteristics of different surfaces, a step-by-step loading test was conducted to determine the limiting PV for each surface. This approach allows for a thorough assessment of

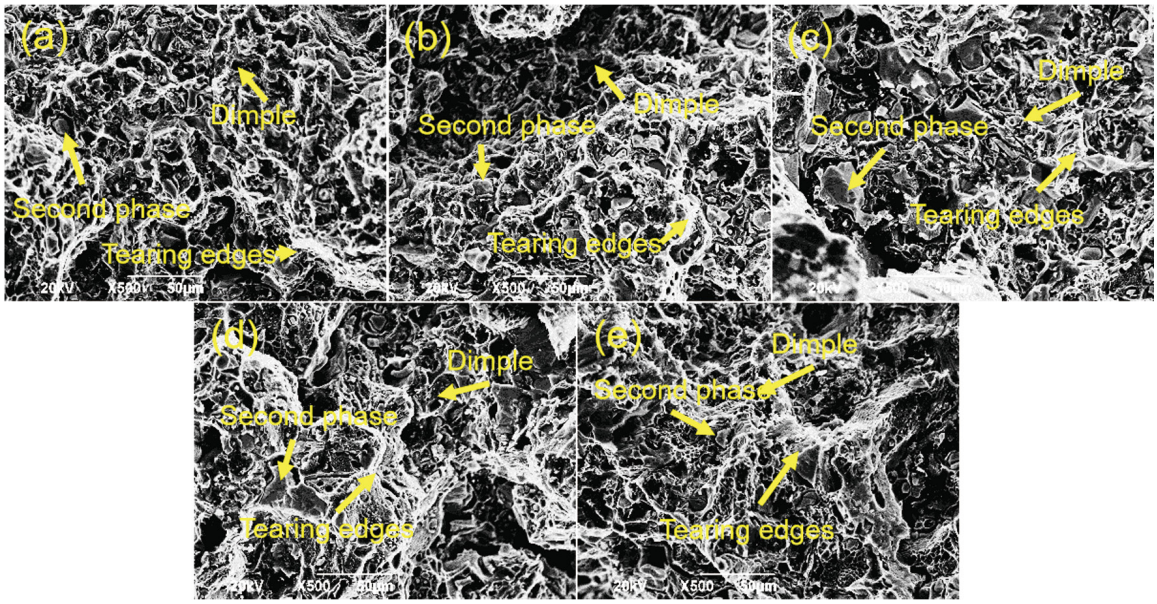

Fig. 12: Fracture morphology of tensile specimens with different surfaces: (a) upper surface; (b) 1/4 surface; (c) 1/2 surface; (d) 3/4 surface; (e) lower surface

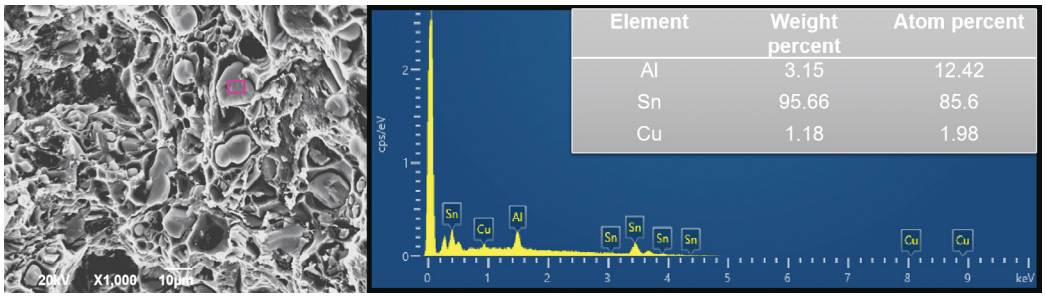

Fig. 13: EDS analysis of second phase microstructure of 1/2 surface tensile test rod fracture

the advantages and disadvantages exhibited by the surfaces in terms of their tribological performance. Figure 14 depicts the development of the friction coefficient as a function of time and load. The results reveal that the tribological characteristics of various surfaces dramatically vary. The tribological performance is the highest on the upper surface. The oil film breakage occurs when the friction coefficient suddenly changes. At this point, the experimental time is approximately 34.3 min, with a load of 3,500 N, and the upper surface has a friction coefficient of approximately 0.011 before failure. Similarly, the 1/2 surface has the worst tribological performance, the test time is approximately 28.3 min, with a load of 2,900 N, and the friction coefficient before failure is approximately 0.047. Furthermore, the lower surface has higher tribological performance, whereas the 1/4 and 3/4 surfaces has nearly identical tribological properties.

To comprehensively analyze the tribological properties of different surfaces, a statistical evaluation was conducted on the average friction coefficient and limit *PV* value changes, as depicted in Fig. 15. This approach provides a more comprehensive understanding of the tribological characteristics exhibited by each surface. The fluctuation trend of the limit *PV* value of various surface samples is identical to that of Sn and Cu segregation and also exhibits a "U"-shaped distribution, but the friction coefficient distribution is opposite to Sn and Cu segregation. Greater Sn and Cu mass percentages correspond to a smaller friction factor and higher limit *PV* value. The observed phenomenon can be attributed to the formation of a protective film on the friction surface through the migration of the molten Sn phase when the temperature increases. This film uniformly distributes itself over the entire contact surface, resulting in a reduction in the friction force [27]. The protective film acts as a lubricant, effectively preventing seizure and minimizing adhesive wear. Furthermore, a higher Sn concentration corresponds to a lower friction coefficient [28]. Meanwhile, the hardness of the casting shows a U-shaped distribution in the direction of thickness. Higher hardness corresponds to greater weight-bearing ability and wear resistance of the alloy. As a result of the step-by-step loading experiment, the upper and lower surfaces have better hardness due to increased Sn and Cu mass fractions, and the samples have good wear resistance, since the friction coefficient of the upper surface is lower and the limit *PV* value is higher.

There are only shallow plow grooves on the upper and lower surfaces and very little wear detritus and no spalling pits. During the friction and wear process, the sample is softer than the abrasive piece and is squeezed and sheared by the load, and some of them fall off the contact surface to create

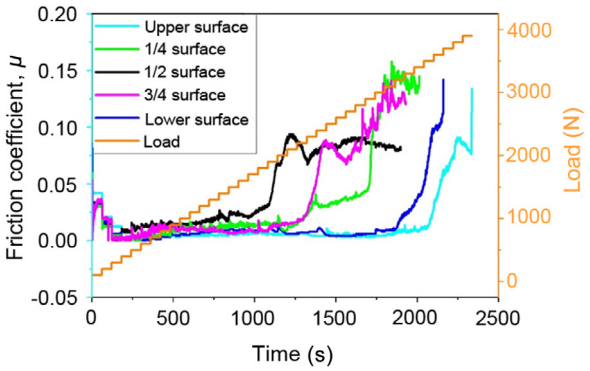

Fig. 14: Results of step by step loading experiment

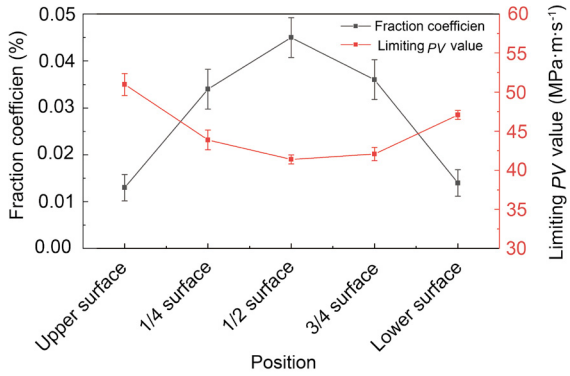

Fig. 15: Curves of average friction coefficient and limit *PV* value of different surfaces

wear debris. When the friction pair rotates and is withdrawn from the contact surface, the other portions remain between the friction surfaces and are repeatedly rolled and hardened by load and relative sliding to generate irregular particles with high hardness. Some of the particles are forced into the aluminum alloy by an external force, and the particles travel with the abrasive piece. During the motion process, the surface of the aluminum alloy undergoes micro-cutting, leading to the formation of plow grooves. Typical abrasive wear morphologies are shown in Figs. 16(a) and (e). Meanwhile, the soft low-melting Sn phase repairs and improves the lubricating oil film and has good anti-friction and anti-adhesion properties, which decreases adhesion and tearing. A higher Cu mass fraction corresponds to a stronger strengthening effect, which improves the bearing capacity of the lubricating film and results in excellent anti-wear and anti-peeling properties. As a result of the elevated Sn and Cu element content on the upper and lower surfaces, the tribological performance of the alloy is enhanced, primarily due to the effective reduction in abrasion and improved wear resistance of the matrix. With a decrease in the mass fractions of Sn and Cu, the hardness and wear reduction effects diminish. This is evident by the presence of visible wear debris and spalling pits on the casting surface, as depicted in Figs. 16(b) and (d). In cases where the Sn and Cu mass fractions reach minimal levels, a distinct surface irregularity characterized by adhesive wear becomes evident, as illustrated in Fig. 16(c).

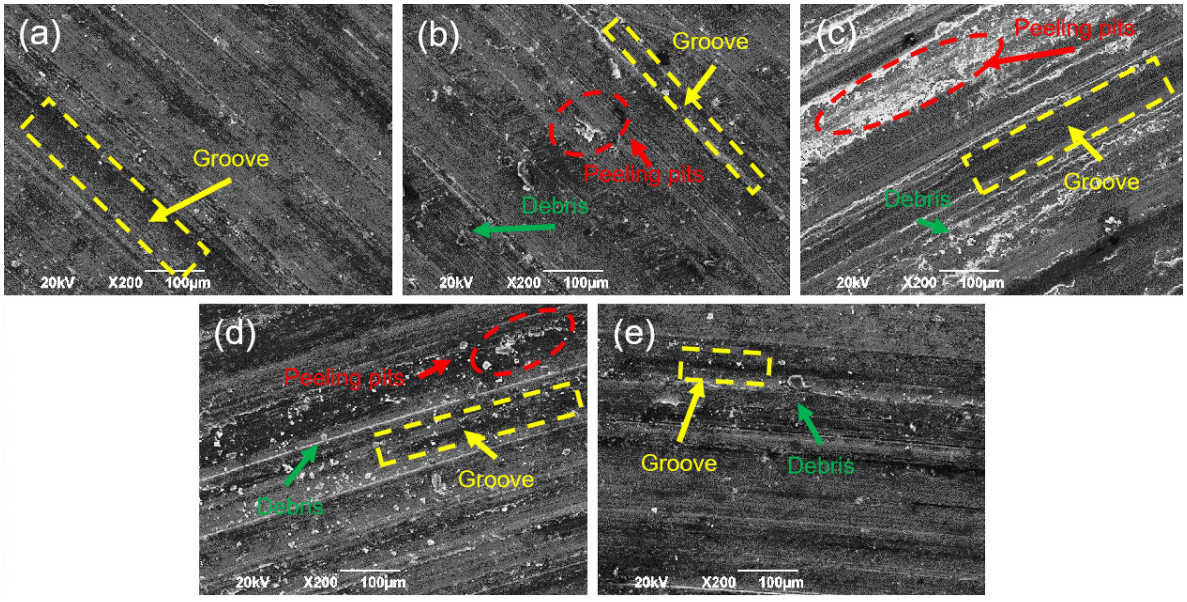

Fig. 16: SEM images of wear marks on different surfaces: (a) upper surface; (b) 1/4 surface; (c) 1/2 surface; (d) 3/4 surface; (e) lower surface

4 Conclusions

(1) Sn and Cu simultaneously segregate in the casting, and the mass fraction of the two elements has a "U" shaped distribution. Furthermore, both positive and negative segregation occur in the casting: positive segregation appear on the upper and lower surfaces, and negative segregation appear on the remaining surfaces; the 1/2 surface (hot node location) has the highest degree of negative segregation.

(2) The synergy of Sn and Cu determins the casting's Vickers hardness, tensile strength, and elongation. Higher Sn and Cu mass percentages correspond to higher hardness, stronger tensile strength, and better elongation.

(3) The findings of the step-by-step loading tests demonstrate that the segregation of Sn and Cu significantly affects the tribological characteristics of the castings. A greater mass fraction of Sn and Cu on the sample's surface results in better tribological characteristics.

Acknowledgements

This research was financially supported by the National Natural Science Foundation of China (No. 51575151 and No. 52005005) and the Science and Technology Project of Anhui Province, China (No. 1501021006).

Conflict of interest

The authors declare that they have no conflict of interest.

References

[1] Kong C J, Brown P D, Harris S J, et al. Analysis of microstructure formation in gas-atomised Al-12wt.%Sn-1wt.%Cu alloy powder. Mater. Sci. Eng. A, 2007, 454: 252–259.
[2] Belov N A, Akopyan T K, Gershman I S, et al. Effect of Si and Cu additions on the phase composition, microstructure and properties of Al-Sn alloys. J. Alloys Compd., 2017, 695: 2730–2739.
[3] Rusin N M, Skorentsev A L, Gurskikh A V. Effect of copper additives on mechanical and tribotechnical properties of sintered composites Al-Sn. Key Eng. Mater., 2016, 685: 295–299.
[4] Felipe B, Emmanuelle S F, Noé C, et al. Microstructure, tensile properties and wear resistance correlations on directionally solidified Al-Sn-(Cu; Si) alloys. J. Alloys Compd., 2017, 695: 3621–3631.
[5] Pathak J P, Mohan S. Tribological behaviour of conventional Al-Sn and equivalent Al-Pb alloys under lubrication. Mater Sci., 2003, 26: 315–320.
[6] Yan N, Hong Z Y, Geng D L, et al. Phase separation and structure evolution of ternary Al-Cu-Sn immiscible alloy under ultrasonic levitation condition. J. Alloys Compd., 2012, 544: 6–12.
[7] Pramanick A, Chaterjee S, Bhattacharya V, et al. Synthesis and microstructure of laser surface alloyed Al-Sn-Si layer on commercial aluminum substrate. J. Mater. Res., 2005, 20(6): 1580–1589.
[8] Perrone A, Zocco A, Rosa H D, et al. Al-Sn thin films deposited by pulsed laser ablation. Sci. Eng. C, 2002, 22(2): 465–468.
[9] Ueda M, Inaba R, Ohtsuka T. Composition and structure of Al-Sn alloys formed by constant potential electrolysis in an $AlCl_3$-NaCl-KCl-Sn-Cl_2 molten salt. Electrochim. Acta, 2013, 100: 281–284.
[10] Noskva N I, Vil'danova N F, Filippov Y I, et al. Preparation, deformation, and failure of functional Al-Sn and Al-Sn-Pb nanocrystalline alloys. Met. Metallogr., 2006, 102(6): 646–651.
[11] Patel J, Morsi K. Effect of mechanical alloying on the microstructure and properties of Al-Sn-Mg alloy. J. Alloys Compd., 2012, 540: 100–106.
[12] Kong C J, Brown P D, Harris S J, et al. The microstructures of a thermally sprayed and heat treated Al-20wt.%Sn-3wt.%Si alloy. Mater. Sci. Eng. A, 2005, 403(1–2): 205–214.
[13] Wu X F, Zhang G A, Wu F F. Influence of Bi addition on microstructure and dry sliding wear behaviors of cast $AlMg_2Si$ metal matrix composite. Trans. Nonferr. Metal. Soc., 2013, 23(6): 1532–1542.
[14] Kotadia H R, Doernberg E, Patel J B, et al. Solidification of Al-Sn-Cu based immiscible alloys under intense shearing. Metall. Mater. Trans. A, 2009, 40: 2202–2211.
[15] Guo H M, Yang X J, Hu B. Low superheat pouring with a shear field in rheocasting of aluminum alloys. J. Wuhan Univ. Technol. Mater. Sci., 2008, 23(1): 54–59.
[16] Li X M, Wang Y, Bi Q C, et al. Experimental study on gas bubble rising velocity in different liquids. J. Xi'an Jiaotong Univ., 2003, 37(9): 971–974.
[17] Liu W, Xing S M, Bao P W. Energy dissipation and apparent viscosity of semisolid metal during rheological processes part II: Apparent viscosity. J. Mater. Sci. Technol., 2007, 23(6): 801–805.
[18] Liu W, Xing S M, Bao P W. Energy dissipation and apparent viscosity of semisolid metal during rheological processes Part I: Energy dissipation. J. Mater. Sci. Technol., 2007, 23(3): 342–346.
[19] Zhong Y, Yan D S, Su G Y, et al. Microsegregation and improving method of a squeeze cast LY12 alloy. Acta Metall. Sin-Engl., 2001, 37(1): 42–46.
[20] Chen F Y, Jie W Q. Study of microsrgregation in Al-Cu-Zn ternary alloys by experiment and scheil model. Acta Metall. Sin-Engl., 2004, 40(6): 664–668.
[21] Zhu C, Zhao Z H, Zhu Q F, et al. Structures and macrosegregation of a 2024 aluminum alloy fabricated by direct chill casting with double cooling field. China Foundry, 2022, 20(1): 1–8.
[22] Wan Q J, Yao H Z. Formation of hot-top segregation in steel ingot and effect of steel compositions. Metall. Mater. Trans. B, 1989, 5(20): 723–730.
[23] Ghomashchi M R, Vikhrov A. Squeeze casting: An overview. J. Mater. Process. Technol., 2000, 101(1–3): 1–9.
[24] Sun J B, Wang X D, Wang S Q, et al. Heat treatment technology of 2A14 alloy extruded bar. Chin. J. Nonferrous Met., 2014, 24(10): 2452–2459.
[25] Sun Y G, Xu Y M. Experimental research on limit [PV] Value of friction pair of hydraulic pump. Hydraulics Pneumatics & Seals, 1994, 3: 9–10. (In Chinese)
[26] Tan Y H. Research on power system of heavy launch vehicle in China. Journal of Rocket Propulsion, 2011, 37(1): 1–6. (In Chinese)
[27] Yuan G H, Li Z J, Lou Y X, et al. Friction and wear characteristics of several Al-Sn-Si-Cu alloys. Tribology, 1998, 18: 151–155. (In Chinese)
[28] Gao Y, Zeng J M, Si J Y, et al. Study on wear-friction bearing properties alloys of Al-Sn. Foundry, 2005, 54(6): 591–594. (In Chinese)